



VU Research Portal

An adaptive temporal-causal network model for decision making under acute stress

Treur, Jan; Mohammadi Ziabari, S. Sahand

published in

Computational Collective Intelligence
2018

DOI (link to publisher)

[10.1007/978-3-319-98446-9_2](https://doi.org/10.1007/978-3-319-98446-9_2)

document version

Publisher's PDF, also known as Version of record

document license

Article 25fa Dutch Copyright Act

[Link to publication in VU Research Portal](#)

citation for published version (APA)

Treur, J., & Mohammadi Ziabari, S. S. (2018). An adaptive temporal-causal network model for decision making under acute stress. In N. T. Nguyen, B. Trawinski, E. Pimenidis, & Z. Khan (Eds.), *Computational Collective Intelligence: 10th International Conference, ICCCI 2018, Proceedings* (Vol. 2, pp. 13-25). (Lecture Notes in Computer Science (including subseries Lecture Notes in Artificial Intelligence and Lecture Notes in Bioinformatics); Vol. 11056 LNAI). Springer/Verlag. https://doi.org/10.1007/978-3-319-98446-9_2

General rights

Copyright and moral rights for the publications made accessible in the public portal are retained by the authors and/or other copyright owners and it is a condition of accessing publications that users recognise and abide by the legal requirements associated with these rights.

- Users may download and print one copy of any publication from the public portal for the purpose of private study or research.
- You may not further distribute the material or use it for any profit-making activity or commercial gain
- You may freely distribute the URL identifying the publication in the public portal ?

Take down policy

If you believe that this document breaches copyright please contact us providing details, and we will remove access to the work immediately and investigate your claim.

E-mail address:

vuresearchportal.ub@vu.nl



An Adaptive Temporal-Causal Network Model for Decision Making Under Acute Stress

Jan Treur^(✉) and S. Sahand Mohammadi Ziabari

Behavioural Informatics Group, Vrije Universiteit Amsterdam,
Amsterdam, The Netherlands

j.treur@vu.nl, sahandmohammadiziabari@gmail.com

Abstract. In recent literature from Neuroscience the adaptive role of the effects of stress on decision making is highlighted. The problem addressed in this paper is how that can be modelled computationally. The presented adaptive temporal-causal network model addresses the suppression of the existing network connections in a first phase as a result of the acute stress, and then as a second phase relaxing the suppression after some time and give room to start new learning of the decision making in the context of the stress again.

Keywords: Adaptive temporal-causal network model
Hebbian learning · Stress

1 Introduction

Stress has a strong impact on both cognitive and affective processes. This impact can be experienced as disturbing, but its main goal is to improve coping with challenging situations. As a bad effect stress may cause some disorders like depression, anxiety or schizophrenia, but as a positive effect it enables individuals to respond to specific types of threats more adequately, keeping an individual's homeostasis up to date and ready for future threats of similar types. In the very first moment of facing the acute stress, an emotional response is triggered which elevates surveillance, perception, and attention on threat-related stimuli [1]. Humans or rodents initially feel incapable or feel they have not any power to control the stress as they do not know how to change the situation and make it better; the stress will be exacerbated in this situation [2]. But it turns out stress also has a positive effect on learning new decision making by suppressing existing connections as a kind of reset and therefore give more room for learning new connections [16]. The current paper addresses the question how this can be modelled by an adaptive computational model.

The paper is organized as follows. In Sect. 2 the neurological principles of the suppressing and adaptive effects of stress and the parts of the brain which deal with stress in that way are addressed. In Sect. 3 the adaptive temporal-causal network model is introduced, and illustrated by simulation of an example scenario. Section 4 addresses the verification of the network model by mathematical analysis. In Sect. 4 the simulation results of the model is declared, in the following section the simulation results and eventually in the last section the discussion of the model is presented.

2 Neurological Principles

Acute stress reactions are considered to involve interaction with the Amygdala [1]. The more activity in the Amygdala, the more an animal becomes sensitive and respondent to the threat [3]. Stressors often deteriorate homeostasis in organisms [4]. But stressors also stimulate a constructive reaction which makes physiological and psychological alterations in the body that are advantageous for the organism. For example, bodily changes in the rapid reaction are going along with amplification of cognitive functions. Recovery from a stressor is accompanied by decreasing negative coupling between the amygdala and the frontal Anterior Cingulate Cortex (ACC) and pre-Supplementary Motor area (preSMA) [5]. This decreasing has been found in stress-related psychiatric disorders [6, 7]. It has been found that the left Prefrontal Cortex (PFC) is relevant to stress adaptation, and individuals with higher Hypothalamic Pituitary Adrenal (HPA) axis reactivity show reduced amygdala-left dlPFC functional connectivity [1]. The PFC and hippocampus in the brain are considered as regions which are responsible for inhibiting the sentimental and unconscious response to fear-inducing stimuli [8]. This relationship reveals that mammals can suppress the threat response if they can fetch up to this result that a stimulus may emerge threatening but it is actually not. In a safe environment, it is advantageous that the cortex has the ability to suppress the stress response but in a harmful environment this may cause a false idea of security [9]. In dangerous conditions, to change the focus to the prospective stress and threats, deployment of energy supplies and consumption is at issue, due to the fact that the brain's vitality utilization (20% of the body's total utilization) is asymmetrical to its size (about 2% of body mass [10]), and the brain has to compete with other body parts to achieving energy and operate for survival [5].

The medial Prefrontal Cortex (mPFC) has power to remove the stress response. Cell fields of the mPFC (by restraining the basolateral amygdala) reduce the effect of emotional responsiveness [11]. And also some parts of the mPFC indirectly hinder the stress response. To decrease a fearful response the ventromedial Prefrontal Cortex (vmPFC) suppresses the amygdala functionality [12]. Neurons in the PFC can put a delay between associated incidents. Hence, time closeness between two stimuli is not necessarily becoming associated. Stress implies that the focus should be in the external world, not on an internal world, and this makes the Amygdala to become hyperactive and PFC and the hippocampus become hypoactive [9]. After inducing stress, the activity of the dorsolateral PreFrontal Cortex (dlPFC), which is a major node of the control network, will be decreased while the activity of Amygdala which is responsible for selecting the stimuli that should be considered first, increased [5].

The reaction of the Amygdala to new stressors makes animals to behave the same as when there was not any earlier stress before the new stress arrived. In [13] it is claimed that the executive control network (by dlPFC), is suppressed in the very starting period of the inducing of stress at the time that catecholaminergic effects overcome corticosteroid increase. Stress handling is viewed as adaptive (e.g., [16]), due to the fact that when their decision making is improved, animals can learn how to change the situation where the stress comes from and release from the threat. In the acute stress, at the very first period of stress-induction, the salience network starts

working and executive control is suppressed. After some period of time, executive control starts performing functionality and suppress the salience network.

3 The Adaptive Temporal-Causal Network Model

To better illustrate and analyze the introduced adaptive network model, the following scenario is addressed here. Person A is working (performing action a_1) in a convenient condition with her colleague B until B's context causes extreme stress for person A. This adverse condition disturbs her normal functioning. Fortunately, A's brain has a mechanism to overcome this by learning new decision making to cope with that situation. By this mechanism, first as a form of reset her existing connections are suppressed to create more room for new learning of connections, better adapted to the new conditions. Next, after some period of time, A's suppression is ending, and new Hebbian learning to cope with the new situation takes place. Finally, after learning how to cope with the stress has accomplished improved decision making, so that instead of working with B, person A decides for a different option (action a_2) in which B and his context does not play a dominant role anymore.

First the Network-Oriented Modeling approach used to model this process is briefly explained. As discussed in detail in [15, Chap. 2] this approach is based on temporal-causal network models which can be represented at two levels: by a conceptual representation and by a numerical representation. A conceptual representation of a temporal-causal network model in the first place involves representing in a declarative manner states and connections between them that represent (causal) impacts of states on each other, as assumed to hold for the application domain addressed. The states are assumed to have (activation) levels that vary over time. In reality, not all causal relations are equally strong, so some notion of *strength of a connection* is used. Furthermore, when more than one causal relation affects a state, some way to *aggregate multiple causal impacts* on a state is used. Moreover, a notion of *speed of change* of a state is used for timing of the processes. These three notions form the defining part of a conceptual representation of a temporal-causal network model:

- **Strength of a connection $\omega_{X,Y}$.** Each connection from a state X to a state Y has a *connection weight value* $\omega_{X,Y}$ representing the strength of the connection, often between 0 and 1, but sometimes also below 0 (negative effect) or above 1.
- **Combining multiple impacts on a state $c_Y(..)$.** For each state (a reference to) a *combination function* $c_Y(..)$ is chosen to combine the causal impacts of other states on state Y .
- **Speed of change of a state η_Y .** For each state Y a *speed factor* η_Y is used to represent how fast a state is changing upon causal impact.

Combination functions can have different forms, as there are many different approaches possible to address the issue of combining multiple impacts. Therefore, the Network-Oriented Modelling approach based on temporal-causal networks incorporates for each state, as a kind of label or parameter, a way to specify how multiple causal impacts on this state are aggregated by some combination function. For this aggregation a number of standard combination functions are available as options and a

number of desirable properties of such combination functions have been identified; see [15, Chap. 2, Sects. 2.6 and 2.7].

In Fig. 1 the conceptual representation of the temporal-causal network model is depicted. A brief explanation of the states used is shown in Table 1.

Table 1. Explanation of the states in the model

X_1	srs_s	Sensory representation of stimulus s
X_2	srs_c	Sensory representation of context c
X_3	srs_{e_1}	Sensory representation of action effect e_1
X_4	srs_{e_2}	Sensory representation of action effect e_2
X_5	fs_{ee}	Feeling state for extreme emotion ee
X_6	ps_{a_1}	Preparation state for action a_1
X_7	ps_{a_2}	Preparation state for action a_2
X_8	ps_{ee}	Preparation state for response of extreme emotion ee
X_9	cs_1	Control state for timing of suppression of connections
X_{10}	cs_2	Control state for suppression of connections

Next, the elements of the conceptual representation shown in Fig. 1 are explained in some more detail. The state srs_s stands for the sensory representation of stimulus s from the world. The state srs_c is the sensory representation of the context c , which is the condition where the acute stress is happening. The sensory representation srs_s of the stimulus is a trigger affecting the activation level of the preparation state of one or both of the actions a_1 or a_2 . The sensory representation of the (predicted) feeling effects of the preparation states ps_{a_1} and ps_{a_2} of the actions are represented by srs_{e_1} and srs_{e_2} , respectively. Furthermore, ps_{ee} is the preparation state of an extreme emotional response on the sensory representation srs_c of the disturbing context c , and fs_{ee} denotes the feeling state associated to this extreme emotion. Finally, cs_2 stands for a control state for suppression of connections and cs_1 for a control state to limit this suppression in time.

The connection weights ω_i in Fig. 1 are as follows. Preparation state ps_{a_1} has three incoming connections from srs_s , srs_{e_1} , ps_{a_2} with weights ω_1 , ω_3 , ω_5 , respectively. The first connection weight ω_1 is for triggering action a_1 during the time that A is working in a convenient condition. Connection weight ω_7 is for the connection for affecting the sensory representation of the feeling effect associated to action a_1 . The negative connection weights ω_5 and ω_6 enable to specify that the two actions exclude each other. Connection weight ω_2 is for affecting activation of the preparation state ps_{a_2} of the second action a_2 when person A makes a new decision, and ω_8 is the weight of the connection to predict the sensory representation of the feeling effect of the preparation state of the second action. Both states srs_{e_1} and srs_{e_2} have two incoming connections from ps_{a_1} , srs_c , and ps_{a_2} , srs_c with weights ω_7 and ω_9 , and ω_8 and ω_{10} respectively. Weights ω_{11} , ω_{12} and ω_{13} are the connection weights for activating the preparation state of the extreme emotion, based on the sensory representation srs_c of the context c , and the feeling state for the extreme emotion, respectively. The connections from cs_2 to

cs_1 and vice versa for timing the suppression have weights ω_{14} , ω_{15} and ω_{16} (negative) which means after some period of time the suppression of the connections will be released by suppressing cs_2 .

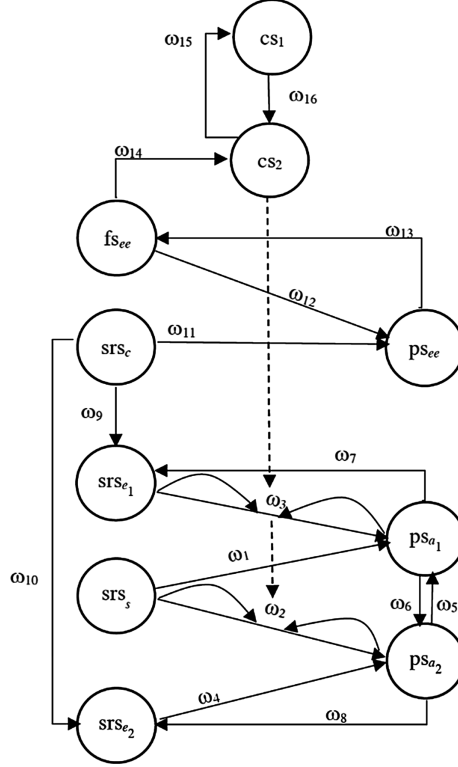


Fig. 1. Conceptual representation of the adaptive temporal-causal network model

This conceptual representation was transformed into a numerical representation as follows [15, Chap. 2]:

- at each time point t each state Y in the model has a real number value in the interval $[0, 1]$, denoted by $Y(t)$
- at each time point t each state X connected to state Y has an impact on Y defined as **impact** $_{X,Y}(t) = \omega_{X,Y} X(t)$ where $\omega_{X,Y}$ is the weight of the connection from X to Y
- The *aggregated impact* of multiple states X_i on Y at t is determined using a *combination function* $c_Y(.,.)$:

$$\begin{aligned} \mathbf{aggimpact}_Y(t) &= \mathbf{c}_Y(\mathbf{impact}_{X_1,Y}(t), \dots, \mathbf{impact}_{X_k,Y}(t)) \\ &= \mathbf{c}_Y(\omega_{X_1,Y}X_1(t), \dots, \omega_{X_k,Y}X_k(t)) \end{aligned}$$

where X_i are the states with connections to state Y

- The effect of **aggimpact** $_Y(t)$ on Y is exerted over time gradually, depending on speed factor η_Y : $Y(t + \Delta t) = Y(t) + \eta_Y[\text{aggimpact}_Y(t) - Y(t)]\Delta t$
or $dY(t)/dt = \eta_Y[\text{aggimpact}_Y(t) - Y(t)]$
- Thus, the following *difference* and *differential equation* for Y are obtained:

$$Y(t + \Delta t) = Y(t) + \eta_Y[\mathbf{c}_Y(\omega_{X_1,Y}X_1(t), \dots, \omega_{X_k,Y}X_k(t)) - Y(t)]\Delta t$$

$$dY(t)/dt = \eta_Y[\mathbf{c}_Y(\omega_{X_1,Y}X_1(t), \dots, \omega_{X_k,Y}X_k(t)) - Y(t)]$$

For states the following combination functions $\mathbf{c}_Y(\dots)$ were used, the identity function $\mathbf{id}(\cdot)$ and the scaled sum function $\mathbf{ssum}_\lambda(\dots)$ with scaling factor λ .

$$\mathbf{id}(V) = V \quad \text{for states with impact from only one other state}$$

$$\mathbf{ssum}_\lambda(V_1, \dots, V_k) = (V_1, \dots, V_k)/\lambda \quad \text{for states with multiple impacts}$$

Similarly, for the connections the following difference equations were obtained. For *Hebbian learning* of a connection from state X_i to state X_j :

$$\omega(t + \Delta t) = \omega(t) + \eta_\omega[\mathbf{c}_\omega(X_i(t), X_j(t), \omega(t)) - \omega(t)]\Delta t$$

with $\mathbf{c}_\omega(V_1, V_2, W) = \mathbf{hebb}_\mu(V_1, V_2, W) = V_1V_2(1 - W) + \mu W$

where μ is the persistence factor with 1 as full persistence. For *state-connection adjustment* with control state cs_2 :

$$\omega(t + \Delta t) = \omega(t) + \eta_\omega[\mathbf{c}_\omega(cs_2(t), \omega(t)) - \omega(t)]\Delta t$$

with $\mathbf{c}_\omega(V, W) = \mathbf{sca}_\alpha(V, W) = W + \alpha V W (1 - W)$

where α (or $\alpha_{cs_2, \omega}$) is the adjustment parameter for ω from cs_2 . In combination these two adaptive combination functions were used as a weighted average as follows:

$$\mathbf{c}_\omega(V_1, V_2, V, W) = \theta \mathbf{hebb}_\mu(V_1, V_2, W) + (1 - \theta) \mathbf{sca}_\alpha(V, W)$$

$$\omega(t + \Delta t) = \omega(t) + \eta_\omega[\mathbf{c}_\omega(X_i(t), X_j(t), cs_2(t), \omega(t)) - \omega(t)]\Delta t$$

All these difference equations were used for simulation. The difference equations for connection weights were applied to connection weights ω_1 and ω_2 for the connections from state X_1 (or srs_s) to X_6 (or ps_{a_1}) and from X_1 (or srs_s) to X_7 (or ps_{a_2}), respectively.

4 Example Simulation

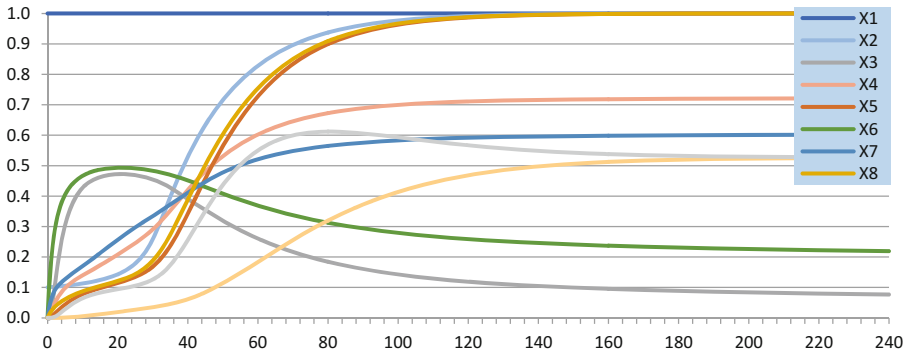
An example simulation of this process is shown in Fig. 2. Table 2 shows the connection weights used, where some of the values are initial values as these weights are adapted over time. The time step was $\Delta t = 0.4$, and weight $\theta = 0.85$. The adjustment parameter α for sca was -0.35 . The scaling factors λ_i for the states with more than one incoming connection are also depicted in Table 2.

Table 2. Connection weights for the example simulation

weight	ω_1	ω_3	ω_5	ω_2	ω_4	ω_6	ω_7	ω_9	ω_8	ω_{10}	ω_{11}	ω_{12}	ω_{13}	ω_{14}	ω_{15}	ω_{16}
value	$\omega_1(0) = 0.9$	0.7	-0.2	$\omega_2(0) = 0.4$	0.7	-0.2	0.7	-0.1	0.7	0.3	1	1	1	1	1	-0.9

state	X_3	X_4	X_6	X_7	X_8	X_{10}
λ_i	0.7	1	2	2	2	1

In the scenario, coping with an extremely stressful condition c (disturbing context of person B) takes place. The trigger for doing one of the actions is the sensory representation state srs_s (also denoted by X_1), which has value 1 all the time. At the early time of working, there is a convenient condition in the working place. Therefore, as can be seen in the Fig. 2, srs_c (also denoted by X_2) has a low value, which, however strongly increases after some time (around time point 30) when the disturbances start. Sensory representation state srs_{e1} (X_3) shows that at that time person A initially has a good feeling for the effect of action a_1 , which strengthens the preparation ps_{a1} (X_6) for this action. However, after time point 30 when the acute stress occurs, this changes. Both the feeling srs_{e1} for the action effect and the preparation ps_{a1} for the action a_1 drop. Moreover, after this time point control state cs_2 (X_{10}), which stands for the control state for suppression of the connections, starts to go up but after some time the other control state cs_1 (X_9) in turn begins to play a role in suppressing cs_2 . Therefore, the actual suppression of the connections mainly takes place between time points 50 and 150. During that time due to the acute stress the connections ω_1 and ω_2 are suppressed by control state cs_2 which is illustrated in the graphs of these two connection weights in Fig. 3. After some time the suppression is released, and by the Hebbian learning person A develops another decision to cope with her task under the extremely stressful condition c . This is shown by increased activation of preparation state ps_{a2} (X_7) in Fig. 2 and by increasing ω_2 (for the connection $X_1 - X_7$) in Fig. 3, in contrast to the decrease of ω_1 (for connection $X_1 - X_6$). Due to this, now the action a_2 is dominating.

**Fig. 2.** Simulation results of working under an extremely stressful condition: states

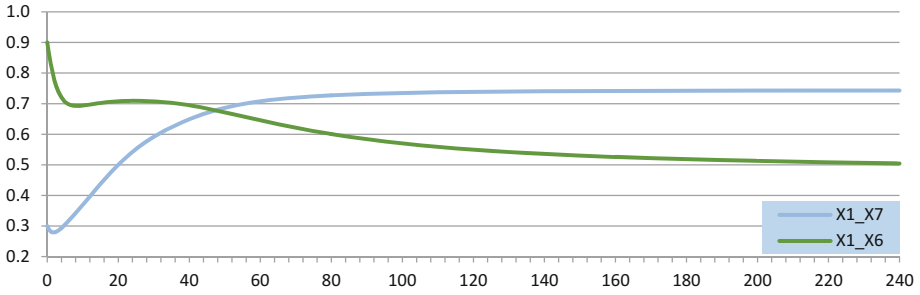


Fig. 3. Simulation results for suppression and Hebbian learning for ω_1 (connection $X_1 - X_6$) and ω_2 (connection $X_1 - X_6$)

5 Verification of the Network Model by Mathematical Analysis

For temporal-causal network models dedicated methods have been developed enabling to verify whether the implemented model shows behavior as expected; see [14, 15, Chap. 12]. In this section in particular the focus is on equilibria: they are determined by Mathematical Analysis and then used for verification by comparison to simulation results. First a definition:

Definition (Stationary Point and Equilibrium)

A state Y in an adaptive temporal-causal network model has a *stationary point* at t if $\mathbf{d}Y(t)/\mathbf{d}t = 0$. Similarly, a connection weight ω in an adaptive temporal-causal network model has a *stationary point* at t if $\mathbf{d}\omega(t)/\mathbf{d}t = 0$. An adaptive temporal-causal network model is in an *equilibrium state* at t if all states and connections have a stationary point at t . In that case the above equations $\mathbf{d}Y(t)/\mathbf{d}t = 0$ and $\mathbf{d}\omega(t)/\mathbf{d}t = 0$ for all states Y and connection weights ω provide the *equilibrium equations*.

The above definition is quite general. However, for adaptive temporal network models the following simple criteria were obtained in terms of the basic elements defining the network, in particular, the states Y , connection weights ω and the combination functions $\mathbf{c}(\cdot)$; see [14, 15, Chap. 12]

Criteria for Stationary Points and Equilibria in Temporal-Causal Network Models

A state Y in an adaptive temporal-causal network model with nonzero speed factor has a stationary point at t if and only if

$$\mathbf{c}_Y(\omega_{X_1,Y}(t)X_1(t), \dots, \omega_{X_k,Y}(t)X_k(t)) = Y(t)$$

where X_1, \dots, X_k are the states with outgoing connections to Y . Similarly, a connection weight ω in an adaptive temporal-causal network model with nonzero speed factor has a stationary point at t if and only if

$$\mathbf{c}_\omega(\alpha_{X_1, \omega} X_1(t), \dots, \alpha_{X_m, \omega} X_m(t), \omega_1(t), \dots, \omega_n(t)) = \omega(t)$$

where X_1, \dots, X_m are the states and $\omega_1, \dots, \omega_n$ the connections with outgoing connections to ω . An adaptive temporal-causal network model is in an equilibrium state at t if and only if for all states and connections with nonzero speed factor the above criteria hold at t .

An equilibrium equation for a scaled sum function

$$\mathbf{c}_Y(\omega_{X_1, Y}(t)X_1(t), \dots, \omega_{X_k, Y}(t)X_k(t)) = (\omega_{X_1, Y}(t)X_1(t) + \dots + \omega_{X_k, Y}(t)X_k(t))/\lambda_Y \\ = Y(t)$$

provides a linear equation

$$\omega_{X_1, Y}(t)X_1(t) + \dots + \omega_{X_k, Y}(t)X_k(t) = \lambda_Y Y(t)$$

in the state values $X_i(t)$ and $Y(t)$ involved. In this way for the network model introduced here the following equilibrium equations for the states were obtained, where are the values for srs_s and srs_c are indicated by A_1 and A_2 (here to simplify notation the reference to t has been left out, and underlining is used to indicate that this concerns state values, not state names).

$$\begin{array}{ll} \text{srs}_s = A_1 & \lambda_4 \text{srs}_{e2} = \omega_8 \text{ps}_{a2} + \omega_{10} \text{srs}_c \\ \text{srs}_c = A_2 & \lambda_8 \text{ps}_{ee} = \omega_{11} \text{srs}_c + \omega_{12} \text{fs}_{ee} \\ \lambda_6 \text{ps}_{a1} = \omega_1 \text{srs}_s + \omega_3 \text{srs}_{e1} + \omega_5 \text{ps}_{a2} & \text{fs}_{ee} = \omega_{13} \text{ps}_{ee} \\ \lambda_7 \text{ps}_{a2} = \omega_2 \text{srs}_s + \omega_4 \text{srs}_{e2} + \omega_6 \text{ps}_{a1} & \text{cs}_1 = \omega_{14} \text{cs}_2 \\ \lambda_3 \text{srs}_{e1} = \omega_7 \text{ps}_{a1} + \omega_9 \text{srs}_c & \lambda_{10} \text{cs}_2 = \omega_{15} \text{fs}_{ee} + \omega_{16} \text{cs}_1 \end{array}$$

This is a set of linear equations in state equilibrium values that can also be written using variables X_1 to X_{10} ; here the naming can be found in Table 1.

$$\begin{array}{ll} X_1 = A_1 & \lambda_8 X_8 = \omega_{11} X_2 + \omega_{12} X_5 \\ X_2 = A_2 & X_5 = \omega_{13} X_8 \\ \lambda_6 X_6 = \omega_1 X_1 + \omega_3 X_3 + \omega_5 X_7 & X_9 = \omega_{14} X_{10} \\ \lambda_7 X_7 = \omega_2 X_1 + \omega_4 X_4 + \omega_6 X_6 & \lambda_{10} X_{10} = \omega_{15} X_5 + \omega_{16} X_9 \\ \lambda_3 X_3 = \omega_7 X_6 + \omega_9 X_2 & \\ \lambda_4 X_4 = \omega_8 X_7 + \omega_{10} X_2 & \end{array}$$

Using the WIMS Linear Solver¹, the following (unique) algebraic solution was obtained for the general case of these equations:

¹ <https://wims.unice.fr/wims/wims.cgi?session=K06C12840B.2&+lang=nl&+module=tool%2Flinear%2Fflinsolver.en>.

$$\begin{aligned}
X_1 &= A_1 \\
X_2 &= A_2 \\
X_3 &= -(A_2(\lambda_6(\lambda_4\lambda_7\omega_9 - \omega_4\omega_8\omega_9) + \omega_5(\omega_{10}\omega_4\omega_7 - \lambda_4\omega_6\omega_9)) \\
&\quad + A_1(\omega_1(\lambda_4\lambda_7\omega_7 - \omega_4\omega_7\omega_8) + \lambda_4\omega_2\omega_5\omega_7)) \\
&\quad / (\omega_3(\lambda_4\lambda_7\omega_7 - \omega_4\omega_7\omega_8) + \lambda_6(\lambda_3\omega_4\omega_8 - \lambda_3\lambda_4\lambda_7) + \lambda_3\lambda_4\omega_5\omega_6) \\
X_4 &= (A_2(\omega_3(\lambda_7\omega_{10}\omega_7 - \omega_6\omega_8\omega_9) + \lambda_3\omega_{10}\omega_5\omega_6 - \lambda_3\lambda_6\lambda_7\omega_{10}) \\
&\quad + A_1(\omega_2\omega_3\omega_7\omega_8 - \lambda_3\omega_1\omega_6\omega_8 - \lambda_3\lambda_6\omega_2\omega_8)) \\
&\quad / (\omega_3(\lambda_4\lambda_7\omega_7 - \omega_4\omega_7\omega_8) + \lambda_6(\lambda_3\omega_4\omega_8 - \lambda_3\lambda_4\lambda_7) + \lambda_3\lambda_4\omega_5\omega_6) \\
X_5 &= -A_2\omega_{11}\omega_{13} / (\omega_{12}\omega_{13} - \lambda_8) \\
X_6 &= -(A_2(\omega_3(\lambda_4\lambda_7\omega_9 - \omega_4\omega_8\omega_9) + \lambda_3\omega_{10}\omega_4\omega_5) \\
&\quad + A_1(\omega_1(\lambda_3\lambda_4\lambda_7 - \lambda_3\omega_4\omega_8) + \lambda_3\lambda_4\lambda_2\lambda_5)) \\
&\quad / (\omega_3(\lambda_4\lambda_7\omega_7 - \omega_4\omega_7\omega_8) + \lambda_6(\lambda_3\omega_4\omega_8 - \lambda_3\lambda_4\lambda_7) + \lambda_3\lambda_4\omega_5\omega_6) \\
X_7 &= (A_2(\omega_3(\omega_{10}\omega_4\omega_7 - \lambda_4\omega_6\omega_9) - \lambda_3\lambda_6\omega_{10}\omega_4) \\
&\quad + A_1(\lambda_4\omega_2\omega_3\omega_7 - \lambda_3\lambda_4\omega_1\omega_6 - \lambda_3\lambda_4\lambda_6\omega_2)) \\
&\quad / (\omega_3(\lambda_4\lambda_7\omega_7 - \omega_4\omega_7\omega_8) + \lambda_6(\lambda_3\omega_4\omega_8 - \lambda_3\lambda_4\lambda_7) + \lambda_3\lambda_4\omega_5\omega_6) \\
X_8 &= -A_2\omega_{11} / (\omega_{12}\omega_{13} - \lambda_8) \\
X_9 &= A_2\omega_{11}\omega_{13}\omega_{14}\omega_{15} / (\omega_{12}\omega_{13}(\omega_{14}\omega_{16} - \lambda_{10}) + \lambda_8(\lambda_{10} - \omega_{14}\omega_{16})) \\
X_{10} &= A_2\omega_{11}\omega_{13}\omega_{15} / (\omega_{12}\omega_{13}(\omega_{14}\omega_{16} - \lambda_{10}) + \lambda_8(\lambda_{10} - \omega_{14}\omega_{16}))
\end{aligned}$$

To compare these outcomes with simulation outcomes, in particular the ones depicted in Figs. 2 and 3, that specific case has been addressed, with parameter values as indicated in Sect. 4, and $A_1 = A_2 = 1$.

$$\begin{array}{ll}
X_1 = 1 & X_6 = -0.1040\omega_2 + 0.7852\omega_1 - 0.1004 \\
X_2 = 1 & X_7 = 0.6760\omega_2 - 0.1040\omega_1 + 0.1524 \\
X_3 = -0.1040\omega_2 + 0.7852\omega_1 - 0.2432 & X_8 = 1 \\
X_4 = 0.4732\omega_2 - 0.07280\omega_1 + 0.4067 & X_9 = 0.5263 \\
X_5 = 1 & X_{10} = 0.5263
\end{array}$$

Now, from the simulation it turns out that in the equilibrium state $\underline{\omega}_1 = 0.5025559926$ and $\underline{\omega}_2 = 0.7428984649$. Substituting this in the above expressions provides:

$$\begin{array}{llllll}
X_1 = 1 & X_3 = 0.0741 & X_5 = 1 & X_7 = 0.6023 & X_9 = 0.5263 \\
X_2 = 1 & X_4 = 0.7216 & X_6 = 0.2170 & X_8 = 1 & X_{10} = 0.5263
\end{array}$$

For verification these state values found by analysis have been compared (in more precision) with the equilibrium state values found in the simulation for $\Delta t = 0.25$. The results are shown in Table 3. As can be seen all deviations are less than 0.001, which provides evidence that the model does what is expected.

Table 3. Comparing Analysis and Simulation

State	srs_s X_1	srs_c X_2	srs_{e_1} X_3	srs_{e_2} X_4	fs_{ee} X_5
Simulation	1.0000000000	0.9999866365	0.0750260707	0.7214675588	0.9999771825
Analysis	1.0000000000	1.0000000000	0.0741370620	0.7216223422	1.0000000000
Deviation	0	-1.33635E-05	0.000889009	0.000154783	-2.28175E-05
State	ps_{a_1} X_6	ps_{a_2} X_7	ps_{ee} X_8	cs_1 X_9	cs_2 X_{10}
Simulation	0.2175996003	0.6021532734	0.9999794070	0.5257977548	0.5267889246
Analysis	0.2169942048	0.6023176317	1.0000000000	0.5263157895	0.5263157895
Deviation	0.000605395	-0.000164358	-2.0593E-05	-0.000518035	0.000473135

Also, for the two adaptive connection weights equilibrium equations can be found. They are:

$$\begin{aligned}\beta_1(X_1X_6(1 - \underline{\omega}_1) + \mu \underline{\omega}_1) + \beta_2(\underline{\omega}_1 + \alpha \underline{\omega}_1(1 - \underline{\omega}_1)X_{10}) &= \underline{\omega}_1 \\ \beta_1(X_1X_7(1 - \underline{\omega}_2) + \mu \underline{\omega}_2) + \beta_2(\underline{\omega}_1 + \alpha \underline{\omega}_2(1 - \underline{\omega}_2)X_{10}) &= \underline{\omega}_2\end{aligned}$$

However, they are not linear and more difficult to be solved algebraically. Nevertheless, they still can be used for verification by substitution of values found in simulations.

$$\begin{aligned}\beta_1 &= 0.85 \quad \beta_2 = 0.15 \quad \mu = 0.8 \quad \alpha = -0.35 \quad X_1 = A_1 = 1 \\ 0.85(X_6(1 - \underline{\omega}_1) + 0.8 \underline{\omega}_1) + 0.15(\underline{\omega}_1 - 0.35 \underline{\omega}_1(1 - \omega_1)X_{10}) &= \omega_1 \\ 0.85(X_7(1 - \underline{\omega}_2) + 0.8 \underline{\omega}_2) + 0.15(\underline{\omega}_1 - 0.35 \underline{\omega}_2(1 - \omega_2)X_{10}) &= \omega_2 \\ X_6 &= 0.217599600251934 \quad X_{10} = 0.526788924575543 \\ X_7 &= 0.602153273449135 \quad \underline{\omega}_1 = 0.502555992556694 \\ \underline{\omega}_2 &= 0.742898464938841\end{aligned}$$

After substitution, the following is obtained:

$$\begin{aligned}0.502214624461369 &= 0.502555992556694 \\ 0.742915691976951 &= 0.742898464938841\end{aligned}$$

The deviations are -0.0003413680953248120 and 0.0000172270381099127 respectively, which both are less than 0.001. This provides evidence that also for the adaptation of the connections the model does what is expected.

6 Discussion

In this paper an adaptive temporal causal network model was presented for the adaptive role of stress in decision making [16]. In this computational model connections are suppressed due to acute stress as a form of reset and Hebbian learning takes place to

adapt the decision making to the stressful conditions. A number of simulations were performed one of which was presented in the paper. Findings from Neuroscience were taken into account in the design of the adaptive model [1, 5, 9, 16]. This literature report experiments and measurements for stress-induced conditions as addressed from a computational perspective in the current paper. In other literature, such as [17] not the Neuroscience perspective is followed, but a more general psychological perspective on decision making. This seems to contrast with the Neuroscience perspective followed in the current paper which is mainly based on [16]. However, the more refined approach on decision making and its subprocesses in [17] such as generation of decision options and selection of an option, may provide interesting inspiration for future research in making a more refined version of the current model. Another future extension may address an explicit role for cortisol in the development of stress. The current states used to model the extreme emotion (ps_{ee} and fs_{ee}) can be seen as aggregate states for a number of brain states, including the cortisol level, but in a more refined approach different substates may be distinguished, under which a separate state for the cortisol level.

Also, a precise mathematical analysis has been done to verify that behavior of our model is as expected. This model can be used as the basis of a virtual agent model to get insight in such processes and to consider certain support or treatment of individuals to handle extreme emotions when they have to work in a stressful context condition and prevent some stress-related disorders that otherwise might develop. In further research, other scenarios can be used and simulated for individuals with different characteristics.

References

1. Quaedflieg, C.W.E.M., van de Ven, V., Meyer, T., Siep, N., Merckelbach, H., Smeets, T.: Temporal dynamics of stress-induced alternations of intrinsic amygdala connectivity and neuroendocrine levels. *PLoS ONE* **10**(5), e0124141 (2015). <https://doi.org/10.1371/journal.pone.0124141>
2. Glass, D.C., Reim, B., Singer, J.E.: Behavioral consequences of adaptation to controllable and uncontrollable noise. *J. Exp. Soc. Psychol.* **7**, 244–257 (1971)
3. Radley, J., Morrison, J.: Repeated stress and structural plasticity in the brain. *Ageing Res. Rev.* **4**, 271–287 (2005)
4. de Kloet, E.R., et al.: Stress and the brain: from adaption to disease. *Nat. Rev. Neurosci.* **6**, 463–475 (2005)
5. Hermans, E.J., Hencknes, M.J.A.G., Joels, M., Fernandes, G.: Dynamic adaption of large-scale brain networks in response to acute stressors. *Trends Neurosci.* **37**(6), 304–314 (2014). <https://doi.org/10.1016/j.tins.2014.03.006>
6. Etkin, A., Prater, K.E., Hoeft, F., Menon, V., Schatzberg, A.F.: Failure of anterior cingulate activation and connectivity with amygdala during implicit regulation of emotional processing in generalized anxiety disorder. *Am. J. Psychiatry* **167**, 545–554 (2010). <https://doi.org/10.1176/ajp.2009.09070931>. PMID: 201123913
7. Johnstone, T., van Reekum, C.M., Ury, H.L., Klain, N.H., Davidson, R.J.: Failure to regulate: counterproductive recruitment of top-down prefrontal-subcortical circuitry in major depression. *J. Neurosci.* **27**, 8877–8884 (2007). PMID: 17699669

8. Morgan, M.A., Romanski, L.M., LeDoux, J.E.: Extinction of emotional learning: contribution of medial prefrontal cortex. *Neurosci. Lett.* **163**, 109–113 (1993)
9. Reser, J.E.: Chronic stress, cortical plasticity and neuroecology, *Behave Process.* (2016). <https://doi.org/10.1016/j.beproc.2016.06.010>
10. Van den Heuvel, M.P., et al.: Functionality linked resting-state networks reflect the underlying structural connectivity architecture of the human brain. *Hum. Brain Mapp.* **30**, 3127–3141 (2009)
11. Figueiredo, H.F., Bruestle, A., Bodie, B., Dolgas, C.M., Herman, J.P.: The medial prefrontal cortex differentially regulates stress-induced c-fos expression in the forebrain depending on type of stressor. *Eur. J. Neurosci.* **18**, 2357–2364 (2003)
12. Sortes-Boyen, F., Bush, D.E.A., Ledoux, J.E.: Emotional preservation: an update on prefrontal-amygdala interactions in fear extinction. *Learn. Mem.* **11**, 525–535 (2004)
13. Barsegyan, A., et al.: Glucocorticoids in the prefrontal cortex enhance memory consolidation and impair working memory by a common neural mechanism. *Proc. Natl. Acad. Sci. U.S.A.* **107**, 16655–16660 (2010)
14. Treur, J.: Verification of temporal-causal network models by mathematical analysis. *Vietnam J. Comput. Sci.* **3**, 207–221 (2016)
15. Treur, J.: *Network-Oriented Modeling: Addressing Complexity of Cognitive, Affective and Social Interactions.* Springer, Heidelberg (2016). <https://doi.org/10.1007/978-3-319-45213-5>
16. Sousa, N., Almeida, O.F.X.: Disconnection and reconnection: the morphological basis of (mal)adaptation to stress. *Trends Neurosci.* **35**(12), 742–751 (2012). <https://doi.org/10.1016/j.tins.2012.08.006>
17. Gok, K., Aatsan, N.: Decision-making under stress and its implications for managerial decision-making: a review of literature. *Int. J. Bus. Soc. Res.* **6**(3), 38–47 (2016)